

# Understanding Three Hydration-Dependent Transitions of Zwitterionic Carboxybetaine Hydrogel by Molecular Dynamics Simulations

Yi He,<sup>†</sup> Qing Shao,<sup>†</sup> Heng-Kwong Tsao,<sup>‡</sup> Shengfu Chen,<sup>§</sup> William A. Goddard, III,<sup>\*||</sup> and Shaoyi Jiang<sup>\*,†</sup>

<sup>†</sup>Department of Chemical Engineering, University of Washington, Seattle, Washington 98195, United States

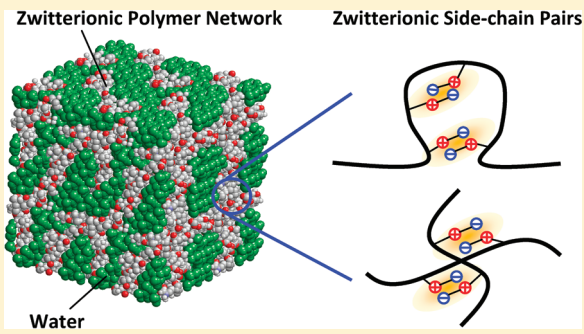
<sup>‡</sup>Department of Chemical and Materials Engineering, National Central University, Taiwan

<sup>§</sup>Department of Chemical and Biological Engineering, Zhejiang University, Hangzhou, China

<sup>||</sup>Materials and Process Simulation Center, California Institute of Technology, Pasadena, California 91125, United States

 Supporting Information

**ABSTRACT:** In this work, molecular dynamics simulations were performed to study a carboxybetaine methacrylate (CBMA) hydrogel under various swelling states. The water content in this study ranged from 28% to 91% of the total weight of the hydrogel. Three transitions of the CBMA hydrogel were observed as the water content increased. The first transition occurs when the water content increases from 33% to 37%. The observed kink in the self-diffusion coefficient of water indicates that the hydration of the polymer network of the hydrogel is saturated; the further added water is in a less confined state. The second transition was found to be related to the physical cross-links of the polymer network. As the water content rises to above 62%, the lifetime of the physical cross-links decreases significantly. This abrupt change in the lifetime indicates that the transition represents the equilibrium swelling state of the hydrogel. Finally, the third transition was observed when the water content goes above 81%. The significant increases in the bond and angle energies of the polymer network indicate that the hydrogel reaches its upper limit swelling state at this transition. These results are comparable to previously published experimental studies of similar zwitterionic hydrogels.



## INTRODUCTION

Hydrogels are water-swollen hydrophilic polymeric networks containing a great amount of water.<sup>1–4</sup> Research on hydrogels, especially the hydrogels made of zwitterionic materials such as carboxybetaine methacrylate (CBMA) and sulfobetaine methacrylate (SBMA), has grown significantly in the past several years.<sup>5–7</sup> This kind of material has unusual physiochemical and optical properties which can be translated into many applications such as enhancing oil recovery,<sup>8</sup> electrophoresis,<sup>9</sup> and electrochemical sensors.<sup>10</sup> One of the unique characteristics of these hydrogels is the existence of zwitterionic cross-links through the electrostatic attractive forces between the opposite charge moieties among two different side chains. These cross-links are directly related to the remarkable phase behavior and solution properties of zwitterionic hydrogels.<sup>11–13</sup> However, the detailed dynamics of these cross-links and their relationship with the swelling states of the hydrogels remain poorly understood.

The molecular dynamics (MD) simulation technique is well suited to provide the detailed structures and dynamics information of systems at the molecular level.<sup>14–16</sup> To the best of our knowledge, MD simulation studies on zwitterionic hydrogels are still not available even though they have been extensively studied

by experimental studies.<sup>17–19</sup> MD simulations on other non-zwitterionic hydrogels are limited as well. These studies have been largely focusing on the structure and dynamics of water and polymer networks in hydrogels. Tamai and co-workers performed molecular dynamics simulations for hydrogel models of poly(vinyl alcohol) (PVA), poly(vinyl methyl ether) (PVME), and poly(*N*-isopropylacrylamide) (PNIPAM).<sup>14,15</sup> They studied the structure and dynamics of hydrogen bonds in the vicinity of the polymer segments. They found that the structure of the hydrogen bonds is stabilized around hydrophilic groups for PVME and PNIPAM. Accordingly, the dynamics of water molecules are highly cooperative with the surrounding polymer chains. They found that both the translational and rotational mobility of water molecules are significantly lower around polymer chains, which is because of not only the hydrogen bonds between the water molecules and hydrophilic groups but also the structuralization of the water molecules around hydrophobic groups, especially for PVME and PNIPAM hydrogels.<sup>14,15</sup> Chiessi et al. further studied the

**Received:** May 19, 2011

**Revised:** August 16, 2011

**Published:** September 06, 2011

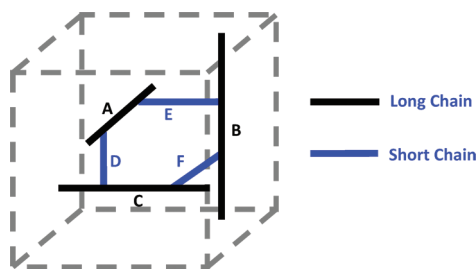


**Figure 1.** Illustration of the network model for hydrogels.

polymer network of cross-linked PVA hydrogels with MD simulations. They found that the local mobility of the PVA polymer network is higher in both the middle of a strand and the proximity of a chemical cross-link than in the rest of the parts.<sup>20</sup>

The properties of hydrogels vary under different water contents. Recently, to investigate the effect of the water content on the polymer network structure and the mechanical properties, Lee and co-workers studied poly(*N*-vinyl-2-pyrrolidone-co-2-hydroxyethyl methacrylate) (P(VP-co-HEMA)) hydrogels with MD simulations.<sup>21</sup> The results showed that the blocky sequence hydrogel exhibits a lower stress level than the random sequence hydrogel due to a more efficiently relaxed VP at low water content.

For zwitterionic hydrogels, two zwitterionic side chains can interact with each other to form inter- or intrachain associations.<sup>12,13</sup> However, it is still not clear what these associations mean in the context of zwitterionic hydrogels, especially when hydrogels are under different degrees of hydration. To further understand zwitterionic hydrogels at the molecular level, we applied an all-atom model to build a polymer network for zwitterionic CBMA hydrogels. The all-atom model is used because detailed descriptions of zwitterionic groups, water, and their interactions inside the hydrogels are desired in this study. The same polymer network was then solvated with different amounts of explicit water molecules to obtain a series of hydrogels under various swelling states. The structural and dynamic properties of water molecules, zwitterionic groups, and the polymer network inside of the hydrogels were then analyzed for each of these swelling states separately.

## SIMULATION MODELS AND DETAILS

The zwitterionic CBMA hydrogel model was built using an approach similar to that reported by Chiessi et al.<sup>20</sup> The model contains a three-dimensional (3D) network structure, as illustrated in Figure 1.<sup>20</sup> The starting polymeric network includes three linear CBMA chains (labeled with A, B, and C in Figure 1). The polymer chains of the network were built with Accelrys Material Studio (version 3.2). Each of these chains has 15 repeating units in a fully extended conformation and a parallel orientation with respect to the Cartesian axes. 1,3-Dioxane cyclic junctions are assumed to be cross-linkers existing in the model. The same cross-linkers were also used in the study by Chiessi et al.<sup>20</sup> There are two 1,3-dioxane cyclic cross-linkers evenly embedded in each chain. These two cross-linkers are separated by 5 CBMA repeating units. Three other linear CBMA chains (labeled as D, E, and F in Figure 1) link the three main chains (chain A, B, and C). Each of them has five CBMA repeating units and is connected to the two different main chains through 1,3-dioxane cyclic cross-linkers so that a network structure is formed. Other cross-linkers such as *N,N'*-methylenebis(acrylamide) and carboxybetaine dimethacrylate cross-linkers can also be used for CBMA hydrogels.<sup>17</sup> A perfect

network structure is assumed in this study. Thus, no structural variations, such as free dangling chain and self-looping, exist in the simulation system. All three main chains in the system participate in forming the network structure through periodic boundary conditions. The final configuration contains six chemical cross-links connecting six CBMA chains.

The polymer network was then solvated with various amounts of water molecules to obtain hydrogels with different water contents. All of the molecular mechanics (MM) and subsequent molecular dynamics (MD) simulations were performed with the LAMMPS (large-scale atomic/molecular massively parallel simulator) simulation package developed at Sandia National Laboratories.<sup>22,23</sup> The equations of motion were integrated using the velocity-Verlet algorithm<sup>24</sup> with a time step of 1.0 fs. The Nose-Hoover temperature thermostat for NVT and NPT MD simulations was used with a damping relaxation time of 0.1 ps. The particle-particle-particle-mesh (PPPM) method<sup>25</sup> was used to calculate electrostatic interactions. All of the systems were initially energy-minimized for 500 000 steps using the conjugate gradient algorithm to remove abnormally close contacts between molecules. After minimization, these systems were equilibrated through 500 ps of NVT MD simulations, followed by 20 ns of NPT MD simulations to obtain the fully relaxed hydrogel systems at 1 atm and 300 K. NPT MD production simulation results from the final 1.0 ns were analyzed to obtain the structure and dynamic properties of water molecules in hydrogels. All data reported in this paper were obtained from two individual MD simulations from two different initial configurations. All simulations were performed on a five-node Intel Quad-Core Beowulf cluster running on Red Hat Enterprise Linux 4.

The all-atom Consistent Valence Force Field (CVFF)<sup>26</sup> was used to describe the interactions in the polymer networks. The partial charges of each atom in the CBMA polymer were calculated using the Jaguar program.<sup>27</sup> Calculations were carried out at the Hartree-Fock (HF) level using the 6-31G\*\* basis set. In this procedure, the electrostatic field at a grid of points was calculated from the HF wave function. Using the grid points outside the VDW radii, atom-centered charges were derived to match the HF potential while reproducing the dipole moment from HF. The water molecules are described with the Extended Simple Point Charge (SPC/E) model.<sup>28</sup>

## RESULTS AND DISCUSSION

To study various swelling states of CBMA hydrogels, the same polymer network was solvated with various amounts of water molecules listed in Table 1. The water content is defined by the mass percentage of water over the total mass of hydrogel. As mentioned before, water, zwitterionic side chains, and the CBMA polymer network are the major focuses of this research. When the water content of the hydrogel was increased from 28% to 91%, three transitions were observed. These transitions were found to be related to the diffusion of water in the hydrogel, the lifetime of zwitterionic side-chain pairs in the polymer network, and the chemical bonds in the CBMA polymer network, respectively.

**1. Transition of CBMA Hydrogel Determined by the Diffusion of Water in the Hydrogel.** It is known from experimental studies that hydrogels contain two types of water molecules: bound and nonbound water.<sup>29,30</sup> At the molecular level, the existence of the two types of water molecules can be distinguished from the self-diffusion coefficient. Figure 2(a) shows the diffusion coefficient of the water molecules in the hydrogels

**Table 1.** Water Contents of CBMA Hydrogels with 60 CBMA Repeat Units

water content of hydrogel (w/w %)	number of water molecules
28%	335
33%	415
37%	502
41%	592
45%	697
49%	819
62%	1396
71%	2120
81%	3630
86%	5250
90%	8200

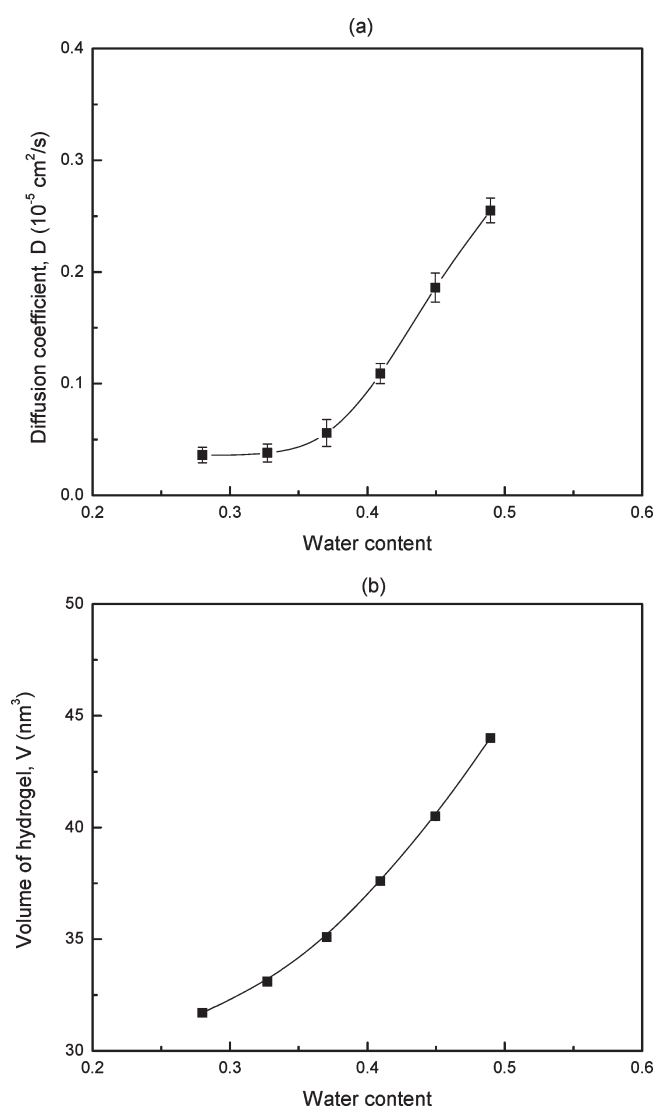


**Figure 2.** (a) Diffusion coefficients of the water molecules in the hydrogels with various water contents. (b) Volumes of hydrogels with various water contents.

as a function of the water content. The diffusion of water molecules in all of these model systems is slower as compared to that



**Figure 3.** Physical cross-linking of zwitterionic polymer chains. (a) Interchain cross-linking. (b) Intrachain cross-linking. The long black curves represent long polymer chains. The short black lines denote chemical bonds. Positively and negatively charged groups are shown in red or blue color, respectively. The cross-linking points are highlighted with orange color.

of bulk water due to the confinement of the polymer network. There is a kink in the diffusion coefficient of water molecules when the water content is increased from 33% to 37%. For comparison, no kink was observed when the volume of hydrogel (each volume was measured after a 20 ns NPT simulation was performed on the hydrogel) was plotted as a function of water content, as shown in Figure 2(b). This indicates that the transition is not solely due to the volume increase of the polymer network. The transition can actually be explained by the existence of bound and nonbound water molecules within the hydrogels. When the water content of the hydrogel is very low (for example, less than 33%), water molecules entering the polymer network will hydrate hydrophilic groups and will bind onto the polymer network. These bound water molecules will have small diffusion coefficients, as they are all in the hydration shell of hydrophilic groups. As long as the hydration shell is not saturated, the diffusion coefficient of water molecules remains stable at a low value. After the hydration shell of hydrophilic groups was saturated with water, some water molecules in the hydrogel will have to stay outside of the hydration shell. Thus, these unbound water molecules can more freely diffuse as compared with those bounded water molecules, leading to the increase in diffusion coefficient.

**2. Transition of CBMA Hydrogel Determined by the Lifetime of Side-Chain Pairs in the Polymer Network.** As the water content continues to increase, the CBMA hydrogel will eventually reach its equilibrium swelling state when its elastic retraction force balances with its swelling force. This equilibrium state refers to the state when a hydrogel was immersed in bulk water. The retraction force comes from chemical and physical cross-links in the polymeric network.<sup>31</sup> Physical cross-links in general may come from entanglements, crystallites, or weak associations such as hydrogen bonds, van der Waals interactions, or electrostatic attractions.<sup>3,12,32</sup> The gel–sol transition of some hydrogels supports the hypothesis that the physical cross-linking is the major driving force for hydrogel formation when chemical cross-linking is absent.<sup>33</sup> Moreover, physical cross-links are subject to changes in surrounding conditions, such as salt concentrations and temperature. Similarly, the equilibrium water content is also sensitive to these changes. This similarity suggests that the lifetime of physical cross-links can be used to identify the equilibrium swelling state of hydrogels. For zwitterionic hydrogels, specifically, it was found that two zwitterionic side chains may associate with each other to form inter- or intrachain associations,<sup>12,13</sup> as shown in Figure 3. These associations can be considered to be physical cross-links which contribute to the retraction force in hydrogels. Therefore, by examining the status

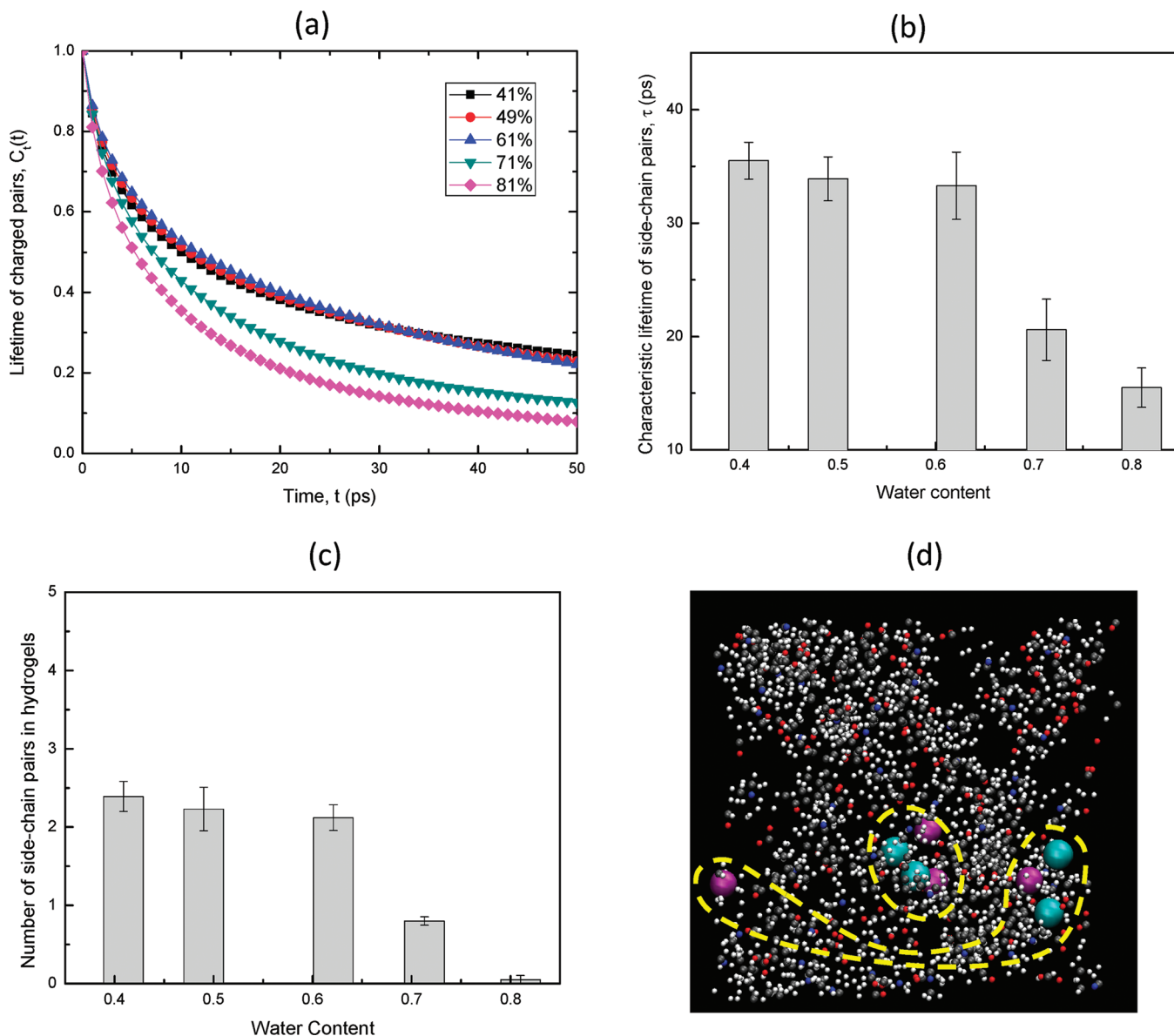


**Figure 4.** (a) Lifetime autocorrelation functions, (b) characteristic lifetimes, and (c) number of side-chain pairs in the CBMA hydrogels at various water contents. (d) A snapshot of the simulation box which shows the zwitterionic side-chain pairs in the CBMA hydrogel which contains 62% water. Red, blue, gray, and white denote oxygen, nitrogen, carbon, and hydrogen atoms in the polymer network, respectively. The carbon and nitrogen atoms in the pairs are shown in the space-fill mode with cyan and purple, respectively. The yellow dashed curves illustrate two zwitterionic side-chain pairs in the hydrogel. Water molecules are not shown. Due to the periodicity of the simulation box, the distance between atoms in a side-chain pair may appear to be far away from each other even though the actual distance between them is very close.

of these associations, it is possible to determine the equilibrium water content of zwitterionic CBMA hydrogels.

In this study, the distance-dependent criterion was used to characterize the zwitterionic physical cross-links in CBMA hydrogels. The threshold distance is 5.5 Å, which was obtained from the first minimum of the radial distribution function of negatively charged groups around positively charged groups. The nitrogen atoms of quaternary amine groups were taken as the centers of positively charged groups, while the carbon atoms of carboxyl groups were taken as the centers of negatively charged groups.

As a physical cross-link, the association between its zwitterionic side-chain pairs should be stable enough so that the hydrogel structure can be maintained. To describe the stability of a physical cross-link, we evaluated the autocorrelation functions

for the lifetime of zwitterionic side-chain pairs from the following expression

$$C_{\text{pair}}(t) = \frac{1}{N_p} \sum_{i=1}^{N_p} \frac{\langle P(0)P(t) \rangle}{\langle P(0) \rangle^2}$$

where  $P(t)$  is a binary function that equals 1 if the zwitterionic side-chain pair exists at time  $t$ ; otherwise,  $P(t)$  equals 0.  $N_p$  is the number of zwitterionic side-chain pairs found in the hydrogel at time  $t$ . The broken brackets ( $\langle \rangle$ ) denote the ensemble average. The definition is similar to that for the lifetime of hydrogen bonding.<sup>34</sup> A slower decay in a lifetime autocorrelation function indicates more stable association between zwitterionic side-chain pairs. In Figure 4(a), we plotted the lifetime autocorrelation

function for the side-chain pairs in the CBMA hydrogels as a function of water content. The results clearly show that the lifetime of zwitterionic pairs decreases quickly when the water content goes above 62%. On the other hand, when water content is lower than 62%, the curves for the lifetime of zwitterionic pairs are almost identical and decay slowly, which indicates the existence of stable associations, i.e., physical cross-linking. To quantitatively measure this difference, the mean lifetime was obtained by fitting an exponential decay function to the  $C_{\text{pair}}(t)$  curve as follows

$$C_{\text{pair}}(t) = A_p \exp\left(-\frac{t}{\tau_p}\right)$$

where  $A_p$  is the amplitude, and  $\tau_p$  is the mean lifetime. The calculated mean lifetime in Figure 4(b) shows that a large decrease in lifetime occurs between 62% water content and 71% water content. This represents the breakdown of physical cross-links inside the hydrogels because of the excessive water existing in the hydrogels, which indicates that 62% is the water content at which the zwitterionic CBMA hydrogel reaches its equilibrium swelling state. This breakdown of zwitterionic physical cross-links was also confirmed by the average number of zwitterionic side-chain pairs of the hydrogels at various water contents. Figure 4(c) shows that the number decreases quickly after 62% water content. The hydrogel model in this study represents a perfectly chemically cross-linked polymer network. Interestingly, the equilibrium water content found in this study is close to the experimentally determined equilibrium water content of a similar CBMA hydrogel with high cross-linker content (100%).<sup>17</sup> Higher cross-linker content usually indicates that the polymer network is closer to being perfectly cross-linked. Carr et al. reported that their hydrogel has an equilibrium water content of ~60%, which is close to the simulation result from this work.<sup>17</sup> Therefore, the lifetime of side-chain pairs can be an alternative approach to determine the equilibrium swelling state of a zwitterionic hydrogel.

**3. Transition of CBMA Hydrogels Determined by Chemical Bonds in the Polymer Network.** When the water content of the CBMA hydrogel was further increased after it reaches its equilibrium swelling state, the third transition was observed. This transition is related to the structure of the polymer network inside the hydrogels. Among four bonded interactions in Figure 5(a), which form the polymer network, the bond and angle interactions are sensitive to the expansion of hydrogels. Figure 5(a) shows that the bond and angle interaction energies have a significant increase when the water content is larger than 81%, while the dihedral and improper dihedral interaction energies do not change much for all of the water contents investigated. Similar changes in four types of bonded energies were also found in Jang's study when a hydrogel was extended in one direction.<sup>16</sup> They observed that the bond stretching energy and angle bending energy of hydrogels increased significantly during the extension. Figure 5(b) shows that the long chains in the hydrogel are fully extended at 81% water content. This suggests that continuous stretching of the polymer chains will increase the bonds and angles of polymer chains away from their equilibrium values, causing significant increases in the bond and angle energies, respectively, as evidenced by higher bond and angle energies for hydrogels at 91% water content relative to 81% water content.

The equilibrium swelling state of hydrogels can be affected by the surrounding conditions, such as salt or temperature. For a hydrogel which has chemical cross-links, the third transition indicates an upper limit for the equilibrium swelling states of the

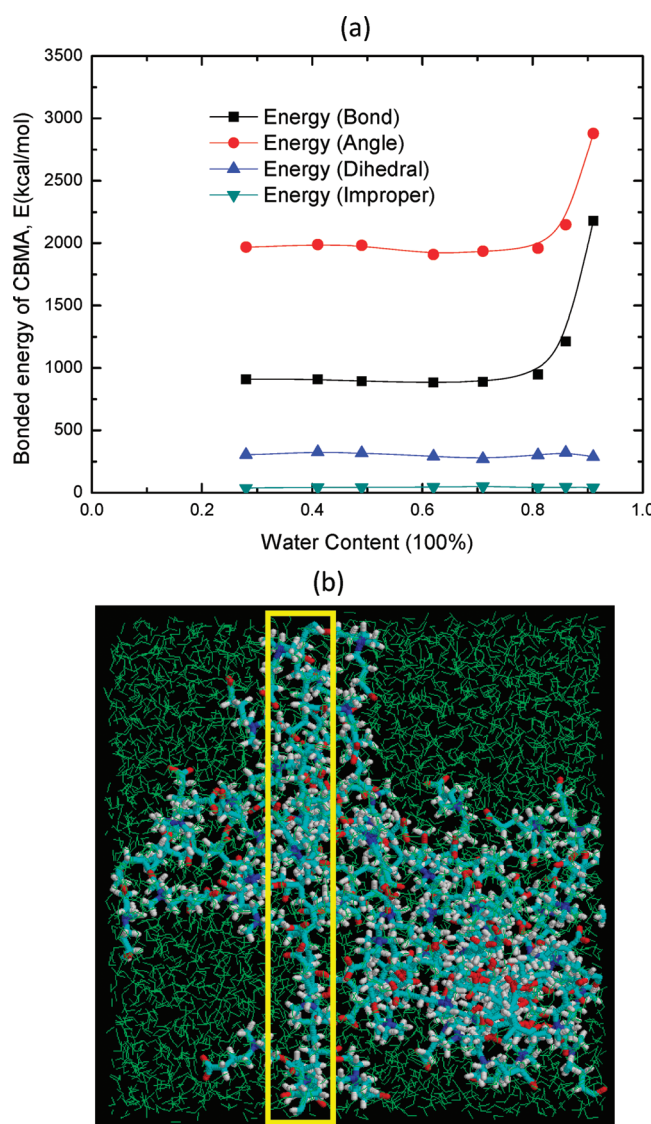


**Figure 5.** (a) Bonded energy of the polymer networks of the CBMA hydrogels at various water contents. (b) A snapshot of the simulation box from the MD simulation of the CBMA hydrogel which contains 81% water. The yellow rectangle shows one of the fully extended chains in the hydrogel. Water molecules are shown with a green wire frame. Red, blue, cyan, and white denote oxygen, nitrogen, carbon, and hydrogen atoms in the polymer network, respectively.

hydrogel, while the chemical bonds remain intact. The existence of an upper limit in the water content of hydrogels was observed experimentally in the study of other zwitterionic hydrogels.<sup>19</sup> It can be explained by how the surrounding conditions affect physical cross-links. For example, Huglin et al. studied the influence of a salt on the water content of poly[*N,N*-dimethyl-*N*-(methacryloyloxy)-ethyl]-*N*-(3-sulfopropyl) ammonium betaine] (pSPE) hydrogels.<sup>19</sup> They found that the water content of pSPE hydrogel varies with salt concentration, with an upper limit of water content at ~90%. The presence of salt ions can cause the expansion of polymer chains by breaking the interchain and intragroup physical associations of poly(sulfobetaines); as a result, the polymer network is able to hold more water until the water content reaches its upper limit.

## CONCLUSIONS

In this work, three transitions were found from a series of MD simulations on CBMA hydrogels at different swelling states. These transitions have distinctive physical meanings. The first transition distinguishes between the two types of water inside hydrogels: bound and nonbound water when the water content increases from 33% to 37%. The second transition shows that the equilibrium water content of CBMA hydrogels can be determined by the change in the lifetime of side-chain pairs. The CBMA polymer network in this work can hold 62% of water at its equilibrium swelling state. Through the examination of the lifetime of physical cross-links in the hydrogel, the current approach can also be extended to identify the equilibrium water content of other hydrogels from simulations. Finally, the third transition shows that the CBMA hydrogel in this study can have a water content up to 81%. The result also indicated that the topology of the chemical bonds of the hydrogel polymer network will affect the upper limit of its equilibrium water content.

## ASSOCIATED CONTENT

**Supporting Information.** Figure S1 and Tables S1 and S3. This material is available free of charge via the Internet at <http://pubs.acs.org>.

## AUTHOR INFORMATION

### Corresponding Author

\*E-mail: sjiang@u.washington.edu; wag@wag.caletch.edu.

## ACKNOWLEDGMENT

The authors wish to thank Louisa Carr for helpful discussion. We would like to acknowledge the American Chemical Society Petroleum Research Funds (ACS PRF #48096-AC7) and the National Science Foundation (CMMI 0758358) for financial support.

## REFERENCES

- (1) Kloxin, A. M.; Anseth, K. S. *Nature* **2008**, *454*, 705.
- (2) Kloxin, A. M.; Kasko, A. M.; Salinas, C. N.; Anseth, K. S. *Science* **2009**, *324*, 59.
- (3) Peppas, N. A.; Huang, Y.; Torres-Lugo, M.; Ward, J. H.; Zhang, J. *Annu. Rev. Biomed. Eng.* **2000**, *2*, 9.
- (4) Langer, R.; Tirrell, D. A. *Nature* **2004**, *428*, 487.
- (5) Zhang, Z.; Chao, T.; Liu, L. Y.; Cheng, G.; Ratner, B. D.; Jiang, S. Y. *J. Biomater. Sci., Polym. Ed.* **2009**, *20*, 1845.
- (6) Xue, W.; Huglin, M. B.; Liao, B.; Jones, T. G. *J. Eur. Polym. J.* **2007**, *43*, 915.
- (7) Susanto, H.; Ulbricht, M. *Langmuir* **2007**, *23*, 7818.
- (8) Soto, V. M. M.; Galin, J. C. *Polymer* **1984**, *25*, 121.
- (9) Righetti, P. G.; Gelfi, C.; Verzola, B.; Castelletti, L. *Electrophoresis* **2001**, *22*, 603.
- (10) Yang, W.; Xue, H.; Carr, L. R.; Wang, J.; Jiang, S. Y. *Biosens. Bioelectron.* **2011**, *26*, 2454.
- (11) Schulz, D. N.; Peiffer, D. G.; Agarwal, P. K.; Larabee, J.; Kaladas, J. J.; Soni, L.; Handwerker, B.; Garner, R. T. *Polymer* **1986**, *27*, 1734.
- (12) Georgiev, G. S.; Mincheva, Z. P.; Georgieva, V. T. *Macromol. Symp.* **2001**, *164*, 301.
- (13) Smilkov, H.; Kamenova, I.; Kamenska, E.; Betchev, C.; Georgiev, G. *J. Mater. Sci.-Mater. Med.* **2008**, *19*, 2389.
- (14) Tamai, Y.; Tanaka, H.; Nakanishi, K. *Macromolecules* **1996**, *29*, 6750.
- (15) Tamai, Y.; Tanaka, H.; Nakanishi, K. *Macromolecules* **1996**, *29*, 6761.
- (16) Jang, S. S.; Goddard, W. A.; Kalani, M. Y. S. *J. Phys. Chem. B* **2007**, *111*, 1729.
- (17) Carr, L. R.; Xue, H.; Jiang, S. Y. *Biomaterials* **2011**, *32*, 961.
- (18) Virtanen, J.; Arotcarena, M.; Heise, B.; Ishaya, S.; Laschewsky, A.; Tenhu, H. *Langmuir* **2002**, *18*, 5360.
- (19) Huglin, M. B.; Rego, J. M. *Macromolecules* **1991**, *24*, 2556.
- (20) Chiessi, E.; Cavalieri, F.; Paradossi, G. *J. Phys. Chem. B* **2007**, *111*, 2820.
- (21) Lee, S. G.; Brunello, G. F.; Jang, S. S.; Bucknall, D. G. *Biomaterials* **2009**, *30*, 6130.
- (22) Plimpton, S. *J. Comput. Phys.* **1995**, *117*, 1.
- (23) Plimpton, S. J.; Pollock, R.; Stevens, M. Particle-Mesh Ewald and rRESPA for Parallel Molecular Dynamics Simulations, *Proceedings of the Eighth SIAM Conference on Parallel Processing for Scientific Computing*, Minneapolis, MN, 1997.
- (24) Swope, W. C.; Andersen, H. C.; Berens, P. H.; Wilson, K. R. *J. Chem. Phys.* **1982**, *76*, 637.
- (25) Hockney, R. W.; Eastwood, J. W. *Computer Simulation Using Particles*; McGraw-Hill International Book Corporation: New York, 1981.
- (26) Dauberoguthorpe, P.; Roberts, V. A.; Osguthorpe, D. J.; Wolff, J.; Genest, M.; Hagler, A. T. *Proteins: Struct., Funct., Genet.* **1988**, *4*, 31.
- (27) Schrödinger, I. *Jaguar*; Portland, OR, 1991–2000.
- (28) Berendsen, H. J. C.; Grigera, J. R.; Straatsma, T. P. *J. Phys. Chem.* **1987**, *91*, 6269.
- (29) Khare, A. R.; Peppas, N. A. *Polymer* **1993**, *34*, 4736.
- (30) Muller-Plathe, F. *Macromolecules* **1998**, *31*, 6721.
- (31) Hoffman, A. S. *Adv. Drug Delivery Rev.* **2002**, *54*, 3.
- (32) Hennink, W. E.; van Nostrum, C. F. *Adv. Drug Delivery Rev.* **2002**, *54*, 13.
- (33) Kowalcuk, J.; Jarosz, S.; Tritt-Goc, J. *Tetrahedron* **2009**, *65*, 9801.
- (34) Rapaport, D. C. *Mol. Phys.* **1983**, *50*, 1151.